Keywords: methane direct injection, gas injector, dual fuel engine, 3D-CFD, SOGAV, PFI, medium pressure direct injection, stratified charge, lambda distribution

3D – CFD Simulation of Direct Gaseous Injection for a Medium Speed Dual-Fuel Engine

Jules Christopher Dinwoodie[1], Sebastian Cepelak[1], Manuel Glauner[1], Pascal Seipel[1], Dr. -Ing. Karsten Schleef[1], Prof. Dr. -Ing. Bert Buchholz[1], Dr. -Ing Martin Theile[2]

[1]University of Rostock, [2]FVTR GmbH

https://doi.org/10.18453/rosdok_id00004649

Abstract

The use of Liquid Natural Gas (LNG) as a fuel theoretically results in around 25% less CO_2 emissions than a diesel engine equivalent. LNG can also be created from biological or synthetic sources as a carbon neutral fuel and there is a large existing onshore infrastructure, making LNG technologies in internal combustion engines a viable option for the road to carbon neutrality. The major problem with its use is methane slip – unburned fuel passing through the engine – as methane is also a greenhouse gas. Using direct injection prevents methane slip during valve overlap. In addition, direct injection can be used to target the fuel away from the cylinder walls and piston top land area, improving efficiency and reducing slip occurring due to incomplete combustion. Using a purely experimental approach it is nearly impossible to gain a thorough understanding of the mixture formation processes within the engine's cylinder. However, through the use of validated Computational Fluid Dynamics (CFD) models these processes can be calculated, analysed and assessed for efficacy.

A gas direct injector has been developed for use on a marine medium-speed dual-fuel methane/diesel engine. CFD was used to characterise the injector's behaviour. The developed CFD models were then applied to the 1/34 DF engine and the mixture formation processes analysed. The series produced low pressure port fuel injector was also modelled and compared with the newly developed medium pressure direct injector. Injection strategies using medium pressure direct injection (MPDI) are presented and conclusions drawn as to the efficacy of using MPDI on a dual-fuel marine engine to reduce harmful greenhouse gas emissions.

Direct gas injection on a four stroke engine of this size is very rare. Most manufacturers rely on low pressure port fuel injection, as high pressure direct injection (HPDI) is costly. Using medium pressure direct injection increases efficiency and power density at a lower price point than HPDI, offering a cost effective and advantageous solution to methane slip in the four stroke dual-fuel marine engine.

1. Introduction

Global shipping continues to grow and the need for low emissions shipping with it. One method of cutting CO_2 emissions by around 25% is the use of dual-fuel LNG/diesel engines, the benefit of LNG being the readily available on-shore infrastructure, the ability of adding drop in syn-LNG in any proportion and the unchallenging handling of the fuel.

The main obstacle to the use of these engines is the issue of methane slip, where unburned methane enters the atmosphere, as methane has a global warming potential of factor 28 over 100 years in comparison to CO_2. If this obstacle can be overcome, dual-fuel methane/diesel engines become a viable option for climate neutral shipping.

Methane slip occurs in turbocharged port fuel injection (PFI) gas engines due to injected methane remaining in the intake manifold and being pushed through the cylinder and out of the exhaust during valve overlap. This form of methane slip is known as shortcutting. Another source is methane slip due to incomplete combustion of methane residing in crevices in the cylinder or flame quenching in near-cylinder wall areas. Much effort has been spent on reducing these crevices to improve combustion efficiency, but the problem of methane shortcutting has not yet been properly addressed.

One method of eliminating methane slip due to shortcutting is by the use of a direct gas injector. Using this technology it is possible to inject methane into the cylinder after exhaust valve closing, effectively eliminating methane shortcutting. This method has not been serially implemented up to now due to the higher costs required for the gas compression. In a world where emissions regulations are becoming increasingly stringent, perhaps it is time to review this strategy as a viable option.

The TEME 2030+ project at the University of Rostock aims to show the potential of this technology using an experimental engine and a custom designed gas direct injector. 3D – CFD simulation supports the design of experiments and custom components for the engine.

In this paper, different operating strategies are presented for using a medium pressure direct injector. These strategies are analysed using 3D – CFD simulations and compared with the serial low pressure PFI injection commonly found in engines of this type.

The results of a cold flow simulation and low pressure PFI injection are fist presented. An approach for homogenous medium pressure direct injection is then examined before options for stratified charge operation are shown.

The simulations show promising results for a low-methane slip operation with improved engine performance, paving the way for the experimental results to follow.

2. Experimental Setup

The experimental engine, injector and optical spray chamber used for injector analysis are presented here, giving an overview of the technology available to the TEME 2030+ project team.

2.1. The Experimental Test Bed & Gas Direct Injectors

The University of Rostock operates one of the largest single cylinder research engines in Europe. This medium speed dual fuel methane / diesel marine engine has a 34 cm bore and a rated power output in excess of 500 kW running at a speed of 720 min^{-1} (generator mode). The engine specifications can be seen in table 1.

Table 1: Technical data of the 1/34 DF single cylinder research engine

Bore	340	mm
Stroke	460	mm
Displacement	41.76	l
Compression ratio	12.75	-
Rated speed	720	min^{-1}
Rated power	> 500	kW
Peak firing pressure	> 200	bar
Pilot fuel System	Decentralised DUAP MPI-CR diesel injector, tilted by 6.5°	-
Max. pilot fuel Pressure	2200	bar
Gas dosing system	Woodward SOGAV 105 / DUAP Gas Direct Injector	
Max. gas Pressure	10 / 600	bar abs
Max. charge air pressure	8.5	bar abs

Load Management

The engine's drive shaft is connected to a 1.2 MW dynamometer to simulate load. The engine is controlled by a freely programmable research engine control unit (ECU) based on the National Instruments PXI platform, allowing online pressure indication and next cycle control. A measurement frequency of 1 Hz is used, with some measurements, such as the in-cylinder pressure, being taken at a frequency of 0.1° CA (crank angle degrees) and synchronized with the crank angle movement. The engine is operated on the generator curve (720 min^{-1}) at different load points, this being the typical application for medium speed marine engines.

Air System

The experimental engine is supplied with compressed air at up to 8.5 bar which is regulated according to the load point of the engine based on the series engine's turbocharger map. Steam can be added to humidify the dry compressed air. To simulate the respective back pressure of a serially produced turbocharger, a system of valves in the exhaust system are opened or closed according to the load point. These technologies allow a great degree of freedom in engine testing, as different turbochargers can be simulated by setting the charge air and back pressures accordingly. An experimental exhaust gas recirculation system (EGR) has recently been installed, allowing EGR rates of up to 30% at 100% load to be realised. An experimental canning for a methane oxidation catalyser (MOC) has also been added, with exhaust gas analysis points before and after the catalyser enabling the performance testing of MOC's. The exhaust gas is analysed using a SESAM i60 Fourier transform infra-red (FTIR) spectrometer, whereby all relevant exhaust gas components can be measured.

Figure 1 represents the infrastructure of the engine test bed.

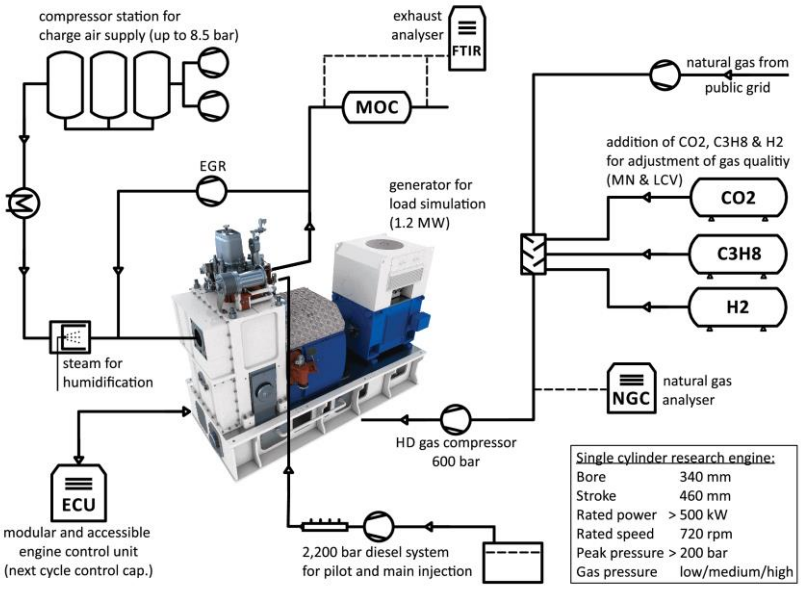

Figure 1: Engine test bed infrastructure

Fuel System

The engine is fitted with a DUAP pilot fuel injector which is decentralised and located between the intake and exhaust valves. The injector is tilted to an angle of 6.5° to compensate for the decentralised position. The four hole nozzle is adapted accordingly. The pilot injector is fed by a common rail system operating at up to 2200 bar. The series engine is fitted with a Woodward solenoid activated gas admission valve (SOGAV) which is located in the intake port and fed by a gas compressor, allowing a maximum gas pressure of 10 bar for port fuel injection (PFI). The natural gas used is taken from the national grid and fed into a mixing unit where propane (C_3H_7) and carbon dioxide (CO_2) can be added, changing the lower heating value and the methane number in order to simulate worldwide LNG qualities. It is also possible to mix in Hydrogen gas (H_2) and experiments have been carried out up to a substitution rate of 80vol%. A novel gas direct injector (DI) was developed within the TEME2030+ project and is mounted centrally in the cylinder head, seen next to the tilted diesel injector in figure 2.

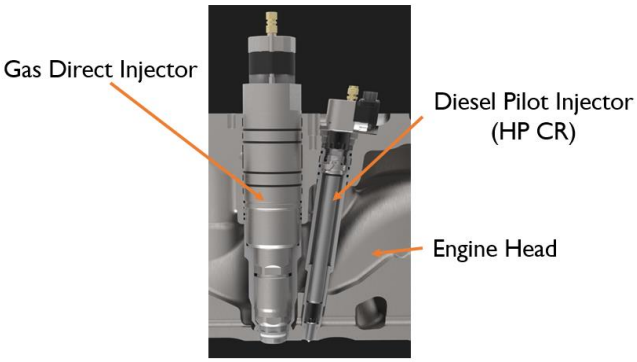

Figure 2: Gas direct injector & DUAP MPI-CR injector in cylinder head

The centrally mounted gas injector was designed by ITAZ GmbH on behalf of DUAP AG using gas simulation calculations over the entire scope of engine operation.

Table 2: Injector Parameters

Cylinder power	450	kW
Standard operating gas pressure range	50 - 80	bar
Maximum gas pressure limit	100	bar
Gas injected at 100 % engine load	4000	mg
Max. injection duration	80	° CA
Min. injection duration	7	° CA
Number of injections per combustion cycle	1 - 2	-
Outer diameter	75	mm
Valve diameter	25	mm
Total injector length	475	mm
Injector weight	22	kg

The gas direct injector is of an outward opening poppet valve type, producing a wide angled hollow cone jet. A jet-forming ring can additionally be installed which bundles the gas into a narrow angled jet. The operating parameters of the injector can be seen in table 2.

The injector is designed for methane or propane gas but addition of hydrogen up to 30vol% is also permissible. Up to 4 g of methane can be injected in up to 80° CA at a gas pressure of 50 to 80 bar at nominal engine speed. The minimum injection duration is 7° CA allowing 2 injections per combustion cycle, if required.

2.2. High Pressure High Temperature Optical Spray Chamber

The University of Rostock also operates a high pressure high temperature optical spray chamber. This consists of a heated and pressurized chamber with a large quartz window. Fuel Injectors are analysed using schlieren photography, whereby changes in the fluid's refractive index are made visible. As

changes to the density directly impact the refractive index of a fluid, this system is also suitable for analysing the flow emitting from a gas injector.

Collimated (laser) light is shone against a mirror at the back of the chamber, where it is reflected back. Changes in the density of the fluid in front of the mirror cause rays to be diffracted. A filter positioned at the reflected light's focal point is used to filter out the original collimated light, leaving the diffracted light to be photographed and hereby make the changes in density visible.

Figure 3 shows the University's optical spray analysis lab and the two measurement positions that will be used to analyse the newly developed gas injector.

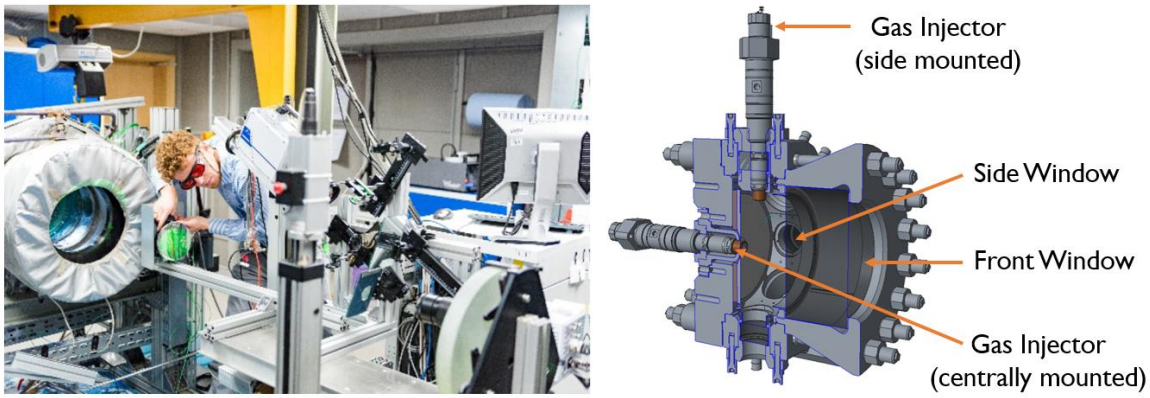

Figure 3: Optical spray analysis lab (left), high pressure high temperature optical spray chamber with gas injectors (right)

This spray chamber was also used for the optical measurement of the diesel pilot injector used in this project.

3. CFD Model

In order to predict the behaviour of the newly designed injector on the serial engine, a CFD model was developed in AVL Fire. Details of the cylinder mesh, system of equations and solver settings can be found in the following section.

3.1. Cylinder Mesh

Structured meshes of the engine's combustion chamber, including intake port, SOGAV, exhaust port and centrally mounted gas direct injector were created using AVL FAME software. The combustion chamber was modelled completely as the cylinder design does not allow for a symmetrical slice approach. The piston top land and threaded hole in the piston centre which is used for installing the piston crown were also modelled as these are recesses in which unburned methane could reside and escape from. Only the valve and nozzle region of the gas injector was modelled, as this has the most influence on the form of the gas injection. Local refinements were added to the near-valve area. The meshes were further refined to correctly resolve the piston top land area and using a time dependent refinement for the diesel spray. A sensitivity study was carried out to determine the most appropriate cell size.

Three cell sizes were chosen, 6 mm for coarse, 4 mm for medium and 3 mm for the fine mesh, resulting in maximum mesh sizes of approximately 1 million, 2 million and 4 million cells respectively. Choosing a smaller cell size results in higher accuracy but at the cost of computational speed, as more time is required to compute the conservation equations for every cell.

Comparison of the gaseous penetration length for the three cell sizes revealed 4 mm to be the most appropriate, as choosing a smaller size results in only a minor change in result, with 4 mm guaranteeing a high degree of accuracy with lower computational time requirements than the fine mesh.

A sample mesh can be seen in figure 4.

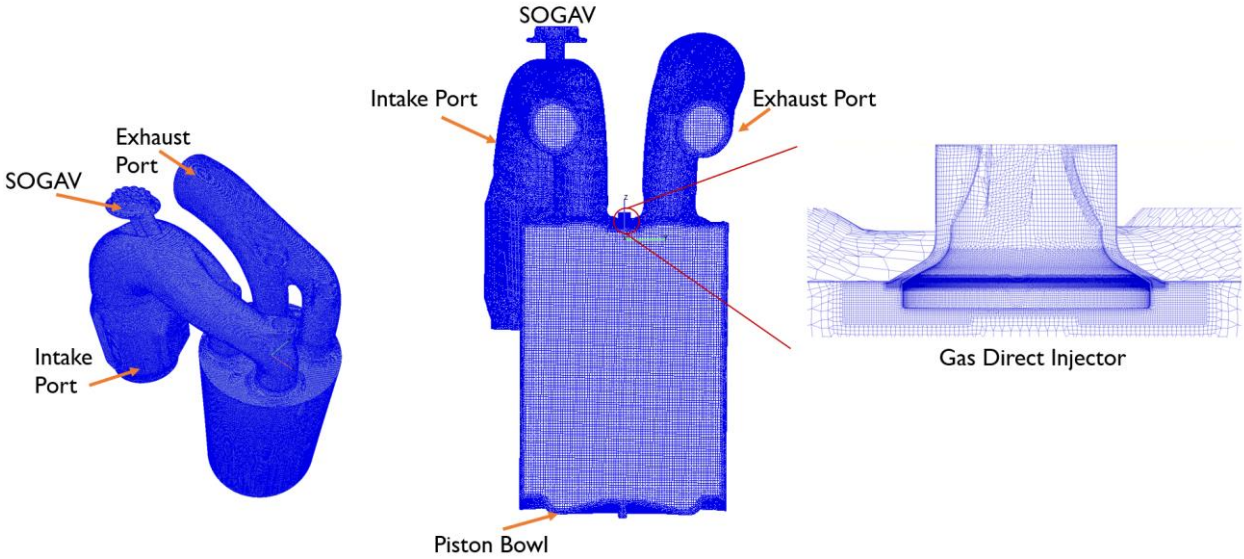

Figure 4: Mesh details showing a) complete mesh (left), b) central cut through mesh (centre) and c) detail of the gas direct injector (right)

As can be seen, the injector nozzle area is very highly refined in order to correctly resolve the sudden expansion of highly compressed gas in the combustion chamber. The resulting cell sizes are 0.25 mm around the injector and 0.0625 mm in a thin band at the exit from the valve seat gap.

3.2. System of equations

The AVL FIRE M solver was used to solve the Reynolds averaged Navier Stokes (RANS) conservation equations for mass, momentum, energy and concentration. Turbulence is modelled using the $k-\zeta-f$ model, a more computationally robust $\overline{v^2}-f$ model, according to Hanjalic, Popovac and Hadziabdic [1]. Due to the high pressures and temperatures within the combustion chamber, the ideal gas equation of state (EOS) has been replaced with the Peng Robinson EOS.

These equations are solved iteratively for every cell of the mesh at every time step to find an appropriate numerical solution and calculate the flow using RANS and the $k-\zeta-f$ modelled turbulence.

3.3. Solver settings and Parameters

The results presented in this paper arise from unsteady, variable time step simulations. The time step was set to 0.5° CA and reduced to 0.1° CA for the injection period using a ramp-up /ramp-down to retain stability. The lower time step was informed by a sensitivity study which was carried out to assess the effect of the time step on the penetration depth.

The calculations were started shortly after exhaust valve opening, allowing exhaust, intake, compression and power strokes to be simulated. The necessary boundary conditions such as wall temperatures and pressures in the inlet/outlet/cylinder were generated from experimental data and

0D/1D simulations. Wall temperatures were set as constant and the walls were treated as non-slip in nature.

The mesh size ranges from 603 000 to 4 million cells depending on the level of refinement (which increases during injections) and the simulated position of the piston. Two boundary layers of 0.2 mm thickness were used to correctly resolve the near wall flow field. During gaseous injection, three finer boundary layers of 0.05 mm thickness are employed due to the high velocity gradient in the wall layers in the direct vicinity of the gas injector.

The gas injection is calculated using a mass flow through the injector's boundary wall. The mass flow is ramped up and down to represent the opening and closing behaviour of the injector. In line with the injector's specifications, a 30° CA injection duration was chosen for the gaseous injection. The diesel pilot injection is treated as diesel EN590 while liquid, evaporating to n-heptane for the dual-fuel combustion model. The discrete droplet mechanism is used, solving differential equations for trajectory, momentum, heat and mass transfer of individual parcels of droplets entering the domain through the nozzle inlet. The droplets are tracked in the Lagrangian manner after an initial blob injection. The Schiller-Naumann [2] drag law has been applied and the Dukowicz evaporation model [3] is used. The initial droplet diameter is set as the diameter of the nozzle hole. Diesel parcels are set to stick to walls and follow a wave-tab secondary breakup scheme. The injected mass is divided into 100 000 parcels over the duration of injection. The diesel spray's breakup length was parametrized by the injector specific breakup time coefficient, based on measurements from previous testing in a high-pressure high-temperature spray chamber.

4. Results

4.1. Validation of the Diesel Spray Model

A separate mesh was created to represent the high-pressure high-temperature spray chamber in which the diesel injector was previously tested (see 2.2), using the same mesh generation parameters as for the cylinder mesh.

The chamber pressure and temperature used in the high-pressure high-temperature spray chamber represent those found in the real combustion chamber at 44° before top dead centre (b.TDC), the timing of the diesel pilot injection. The 75 mg diesel injection is equivalent to the amount used in engine testing at full load, ensuring that the results from the spray test and simulation are directly transferable to the full engine model. As the injector has an asymmetric spray, the entire spray chamber was modelled. The mesh size was 2.2 million cells. The injector specific breakup length parameter was varied in a series of simulations to fit with the experimental results. The best fit being found at a value of 260, as can be seen in figure 5.

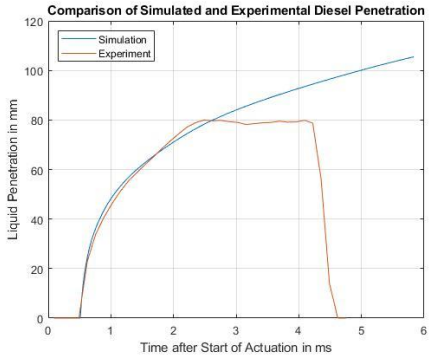

Figure 5: Comparison of Simulated and Experimental Diesel Penetration, liquid phase

The simulated diesel penetration follows the experimental well from the start of actuation, although there are anomalies in the experimental results due to the movement of the physical needle, meaning that the mass flow is not constant as in the simulated results. This explains the slight over- and under-shooting up to around 2.6 ms.

Following this initial period, the simulated results overshoot the experimental results. This is to be expected, as information about all injected parcels is stored and the maximum penetration calculated from this information. The optical measurement equipment, however, cannot track every single droplet, meaning that the simulated penetration length is expectedly higher than the experimental.

There is, however, a large discrepancy in the evaporation of the diesel, seen in the experiment at around 4.3 ms after the start of actuation. By 4.6 ms all the diesel has evaporated, seen in the fact that the liquid penetration length is zero. In the simulated result, a significant amount of the diesel remains liquid, evaporating much later than in the experiment.

The form of the diesel spray was also well reproduced by the simulation, as can be seen in figure 6.

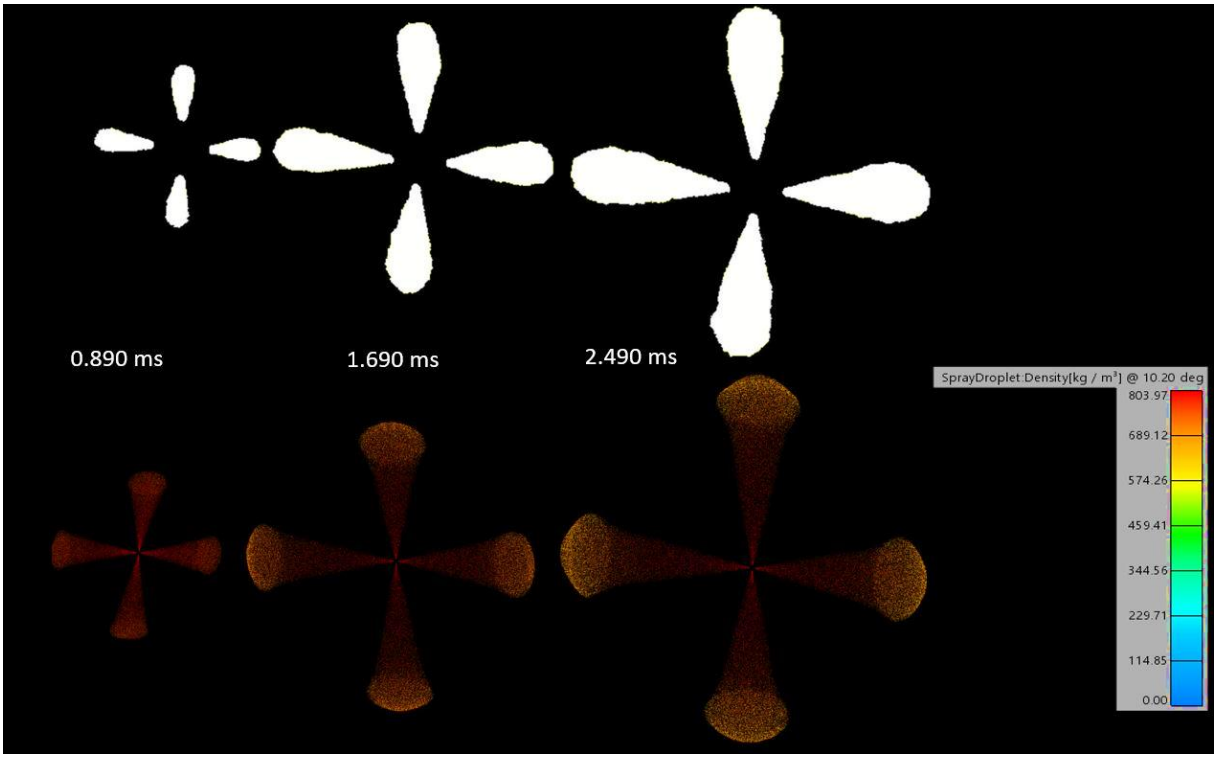

Figure 6: Comparison of experimental diesel sprays (shadowgraph, white, above) with simulated spray results, visualized using density (lower row)

There is more turbulence to be seen on the shadowgraph outline than is evident in the simulation, the reason being that the simulated results consist of droplets and not of a sheet-like diesel front which is perturbed by the surrounding air. The central portion of the diesel sprays are missing in the shadowgraphs as the mirror is obscured by the injector in this location.

The simulated results show good agreement with the measured ones, allowing the spray model to be successfully validated.

4.2. Validation of the CFD Engine Model by Cold Flow Simulation

A cold flow simulation consisting of exhaust, intake, and compression stroke was carried out and the resulting pressure trace compared with the measured pressure trace from the experimental engine. The results are shown in figure 7.

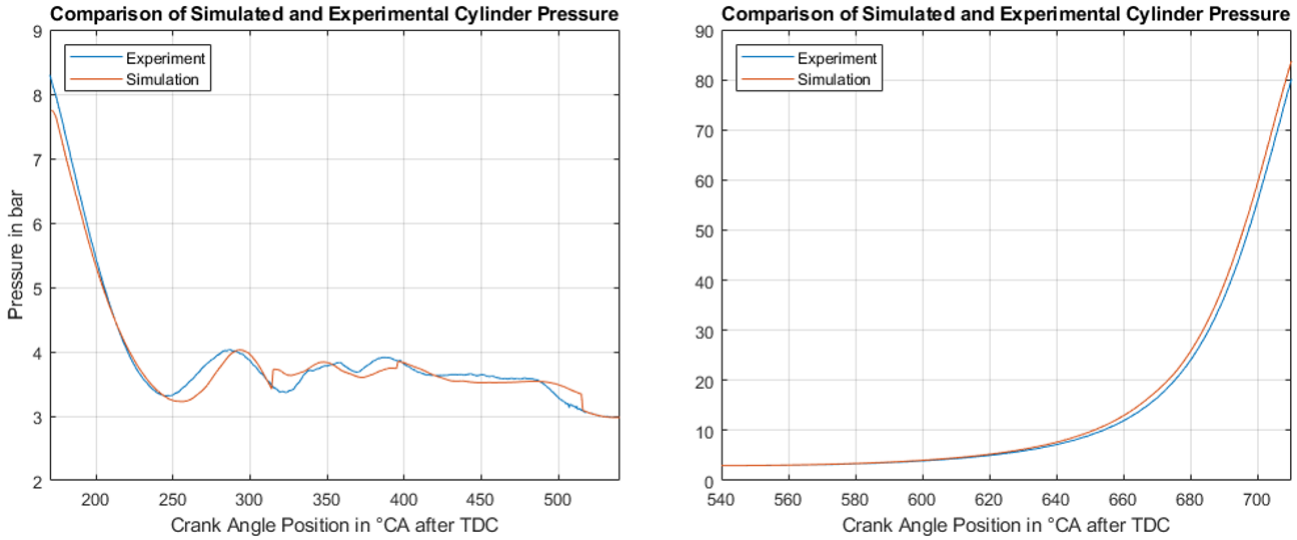

Figure 7: Comparison of experimental and simulated cylinder pressures

In general, the simulation produces good results and a very comparable pressure trace. The simulated results are not as highly refined as the experimental ones, resulting in the slightly more jagged appearance of the pressure oscillations between 170° CA and 540° CA after top dead centre (a.TDC). In the simulated result, pressure is lost more rapidly through the exhaust valve, as seen between 170° CA and approx. 240° CA. From around 640° CA, the simulated cylinder pressure is higher than the experimental results. A comparison of the mesh volume at bottom dead centre (BDC) and top dead centre (TDC) confirmed the accuracy of the mesh, giving a simulated compression ratio of 12.7495 in comparison with the experimental engine's 12.75.

At 710° CA a.TDC, the simulated cylinder pressure is 3.72 bar higher than the measured pressure. The simulation does not take blowby and leakage into account, however. An overall leakage of 3% cylinder mass would lead to a pressure drop of 3.3 bar. This leakage is high, but not impossible taking all the leakage sources into account. Another explanation for the discrepancy is the engine's compression ratio not being quite as stated in the specifications. A combination of these two factors and the low level of discrepancy accompanied by the comparability of the pressure traces make the simulated results feasible.

4.3. In Cylinder conditions

An understanding of the in cylinder conditions is essential in order to fully understand the mixing processes, as turbulence, tumble, swirl, and cylinder filling all have a role to play.

Analysis of Gas Exchange

The gas flow during the exhaust stroke, valve overlap and intake stroke is analysed using a series of plane cuts as shown in figure 8.

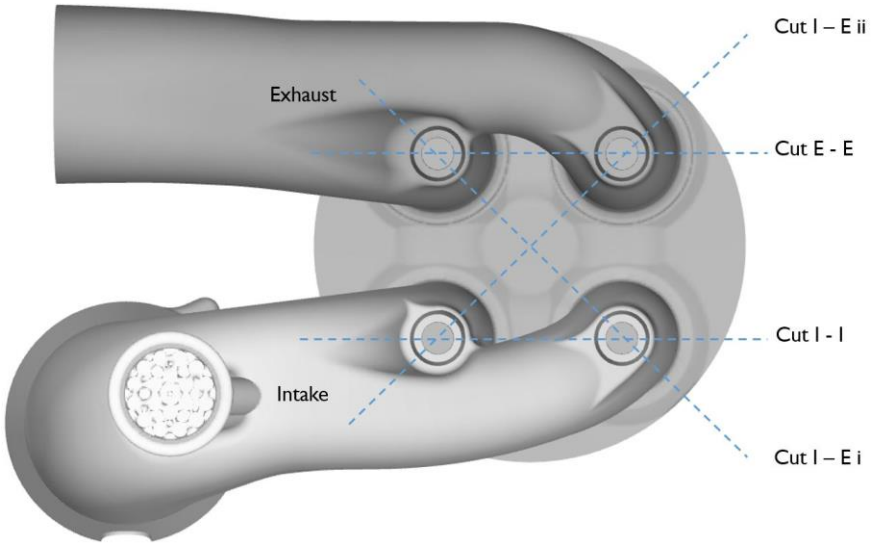

Figure 8: Position of cutplanes for analysis of gas exchange

A cutplane is laid through the centre plane of the two intake valves (cut I – I) and another through the central plane of the exhaust valves (cut E – E). Two further cuts are placed through the central plane of the cylinder, intake and outlet valves (cuts I – E i and I-E ii).

The simulation was started with a stationary flow field at 550° CA b.TDC, within the exhaust stroke. The upwards movement of the piston and the pressure difference between cylinder and exhaust manifold give the potential required to start the flow through the exhaust valves.

At this point the exhaust and cylinder are filled with exhaust gases. The mass fraction of CO_2 is 0.071, as expected for an air-fuel ratio (λ) of 2.2. The flow field demonstrates a relatively uniform character, the flow being oriented bottom to top and with a slight tilt towards the open exhaust valves.

These characteristics continue up the opening of the intake valves at 404° CA b.TDC. By this time, the exhaust valve is well opened, the intake valve is just opening. The flow field is still directed towards the exhaust as the intake valve opens. The highest velocities arise in the narrow intake valve seat gap. The fresh air entering the cylinder is entrained in the exhaust gas flow. In a turbocharged dual fuel engine with PFI, methane slip by shortcutting during valve overlap would occur here, as the fresh air and methane retained in the intake manifold is carried into the exhaust manifold. The exhaust valve closes at 326° CA b.TDC, shown in figure 9.

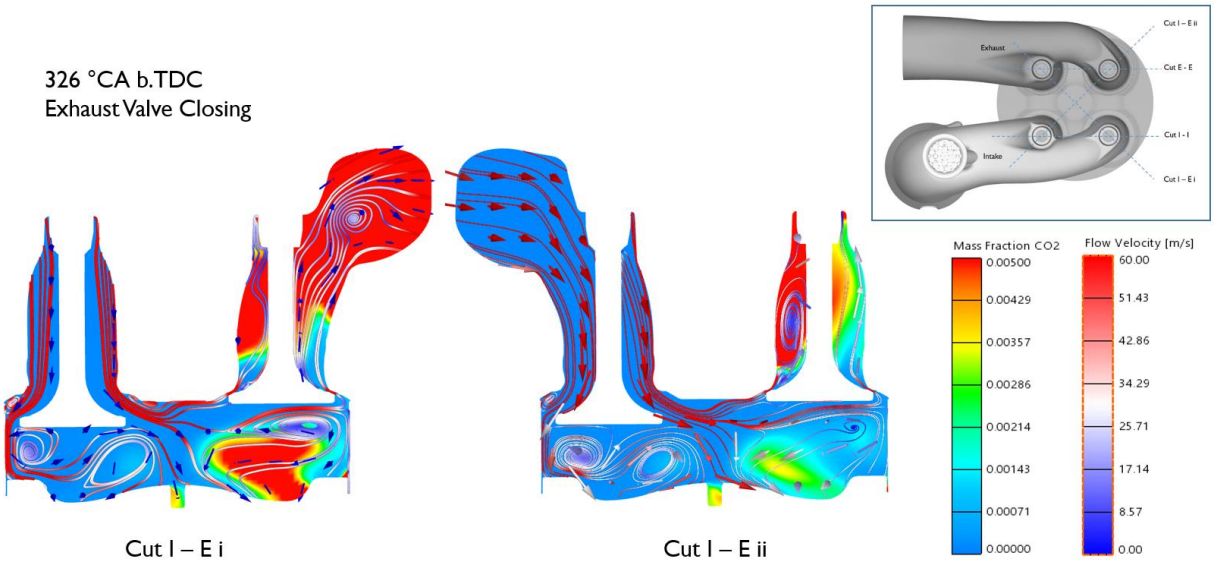

Figure 9: Flow field and CO_2 mass fraction at exhaust valve closing, cutplanes I – E

There is a small amount of exhaust gas that cannot escape the cylinder and is retained in the piston bowl below the exhaust valves. The red areas of the cutplanes indicate cells where the mass fraction of CO_2 is 0.005 (0.5%) or higher. This is caused by the flow emanating from the intake valves pushing the exhaust gas into this pocket while fresh air bypasses the cylinder. Vortices are also observed under both intake and exhaust valves. The flow field at intake valve closing is shown in figure 10.

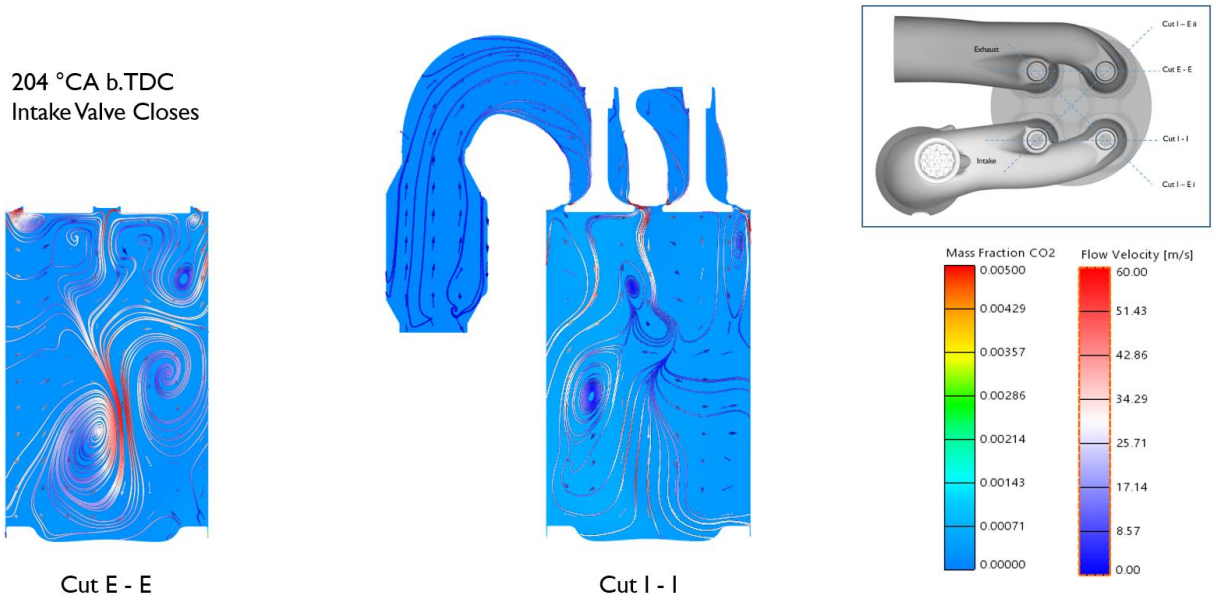

Figure 10: Flow field and CO_2 mass fraction at intake valve closing

The remaining exhaust gas is quite well dissipated by now, although the mix is not completely homogenous. As the intake valves close, the overall velocity of the incoming fresh charge is reduced, creating less dense and slower moving vortices. The highest velocities are found in the intake valve seat gaps and at the meeting of two downwards directed flows in cut E - E, creating two opposed spin vortices. The spin on the right hand side of cut E - E is largely counter clockwise, on the left hand side

mainly clockwise. This flow pattern is also represented on the intake side, as seen in cut I – I. This omega tumble can also be observed in the intake – exhaust cutplanes, not shown here.

Swirl

Cutplanes across the z-axis were also taken through the cylinder, 30 mm below the head. This position was chosen as it is within the engine's clearance volume, making it visible at any engine operation point. The results of the flow field and EGR mass fraction analysis can be seen in Figure 11.

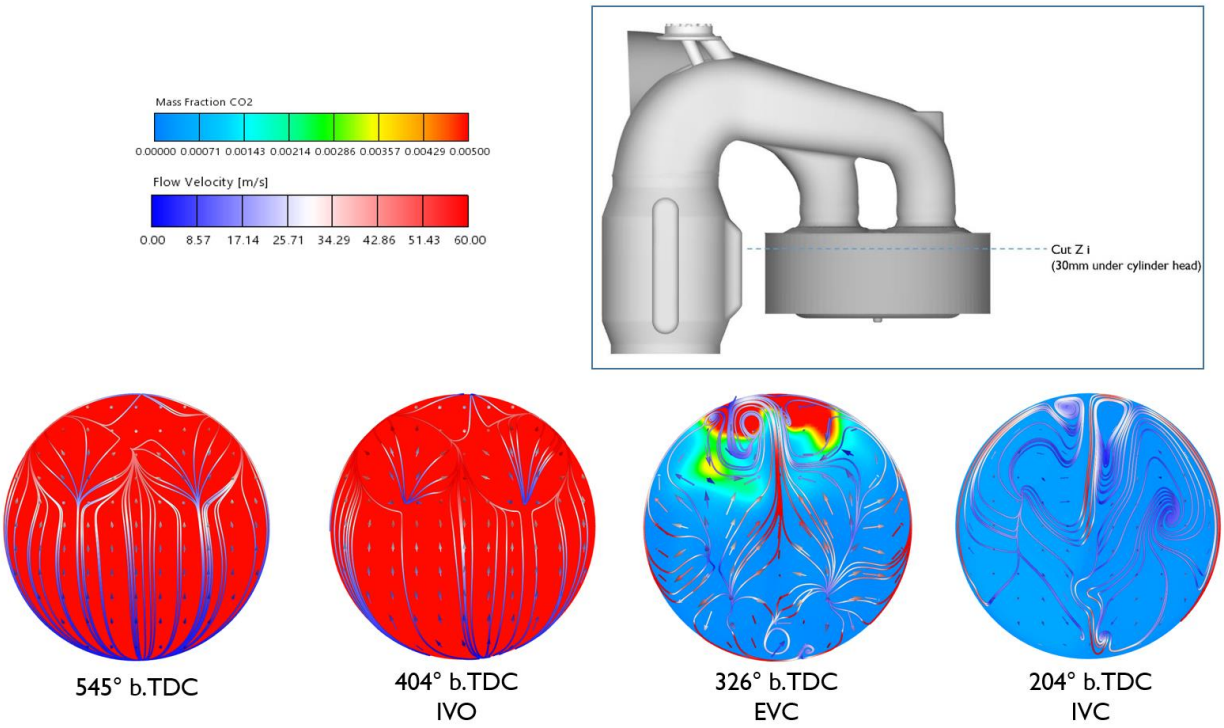

Figure 11: Cross-cylinder and swirl flow

Between 545° and 404° CA b.TDC cross flow from the intake side of the cylinder (bottom of circle) to the exhaust side (top) can be observed. This has a uniform direction, whereas the flow patterns shown from 326° b.TDC exhibit different behaviour. At exhaust valve closes (326° b.TDC) there is a central flow from intake to exhaust side, a counter clockwise flow on the right hand side and a clockwise flow on the left hand side which converge in the middle and slightly to the left of the mid-point of the two exhaust valves. At IVC (205° b.TDC) the flow seems to exhibit a low velocity omega swirl form, with the fresh air flowing along the sides of the chamber (right hand side: counter clockwise; left hand side clockwise) and returning in the middle (top to bottom).

Having now analysed the flow processes, the serial low pressure PFI operation is compared with alternative operation strategies using a medium pressure direct injector.

4.4. Low pressure PFI Operation

The serial low pressure PFI mixing process is examined here, allowing a comparison between conventional operation and operation with a medium pressure direct injector. The simulation was based on experimental results at 100% load. The mean indicated pressure was 20.4 bar, the charge air pressure 4.03 bar. The intake and exhaust pressure traces were used as boundary conditions for the inlet and outlet.

Figure 12 shows the location of the cutplane used for the examination of the PFI mixing process.

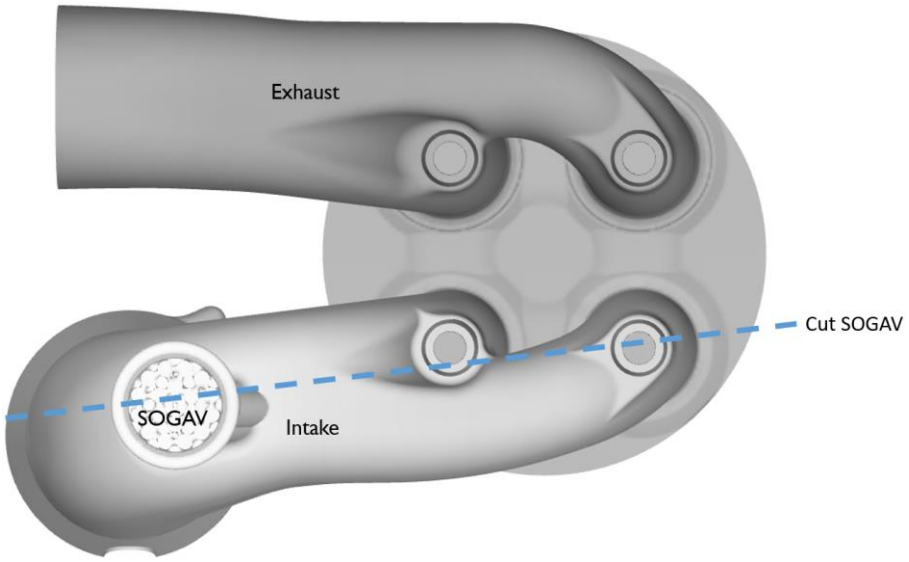

Figure 12: Location of cutplane for the examination of the low pressure process

A cutplane is taken across the two intake valves and the intake manifold including the SOGAV injector, showing the mixing of methane and air in the intake port and the admission of this mixture into the engine's cylinder.

In the low pressure process, methane is injected into the intake stroke between 361° b.TDC and 296° b.TDC, as seen in figure 13, visualised by the mass fraction of methane.

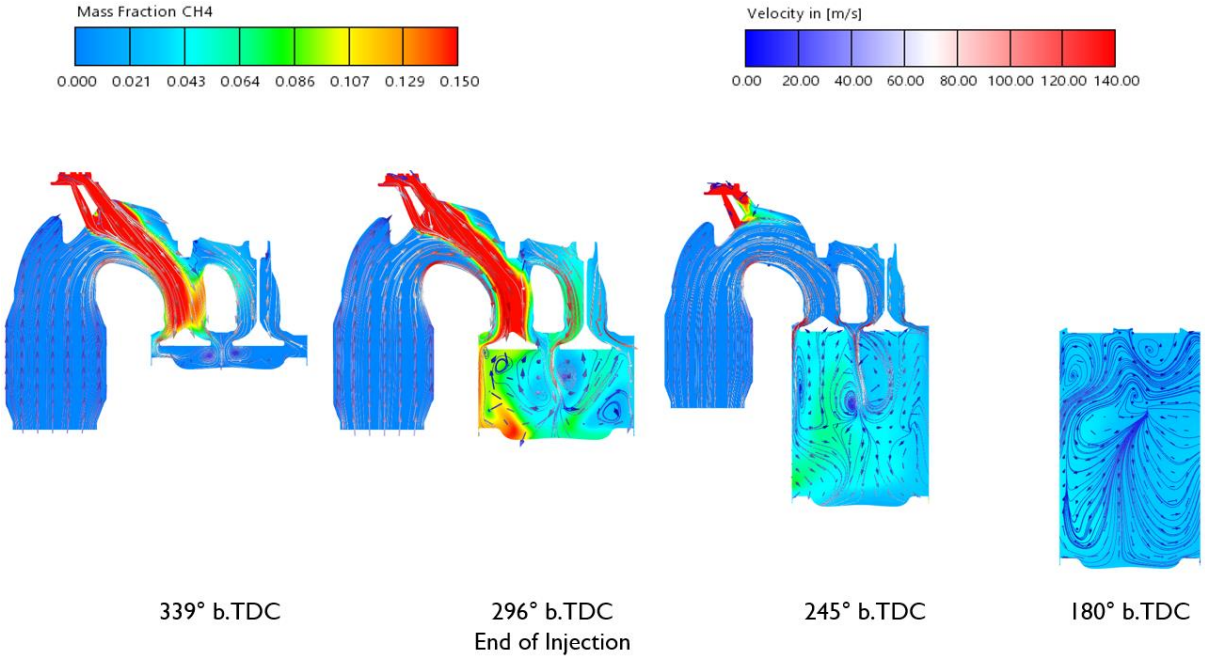

Figure 13: Injection of methane using a SOGAV injector at 100% load

At 361° b.TDC, the SOGAV injector is opened, admitting methane into the intake port. It takes around 20° CA for the methane to reach the left hand intake port, shown here at 339° b.TDC. The fuel travels through the intake manifold in a tight tube-like formation, primarily entering the combustion chamber

via the left hand intake valve, as shown at 296° b.TDC. The majority of methane is admitted via the intake valve closest to the intake manifold (left hand side). This behaviour is corroborated by independent simulations of the M34DF mixing process in [5], who found that 63% of fuel was admitted via the intake valve closest to the intake manifold – in figure 13 the left hand valve. Towards the end of injection, methane predominantly enters the cylinder on the left hand side of the left hand valve, travelling along the cylinder wall and into the piston bowl. Although the injection is completed at 296° b.TDC, methane from the intake port continues to enter the cylinder. This has largely ceased by 245° b.TDC. Fuel gas however still remains in the intake manifold and SOGAV bores until intake valve closing at 205° b.TDC. This methane will remain in the intake manifold until the next cycle, where it could be lost as methane slip though the exhaust valve during valve overlap. At 180° b.TDC, the mixture appears quite well homogenised, with a slightly richer area on the side of the cylinder closest to the intake manifold. Further homogenisation will take place in the compression stroke, as shown in figure 14.

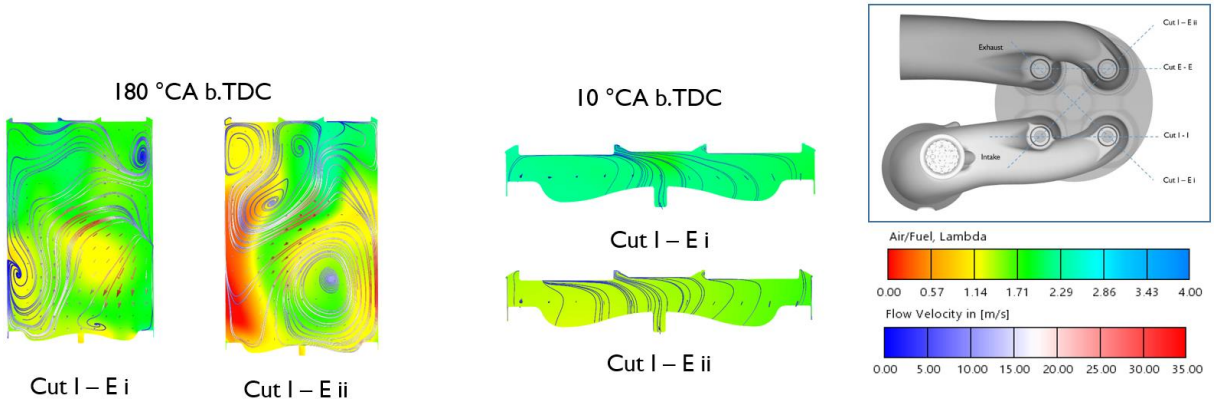

Figure 14: Homogenisation in the compression stroke, low pressure SOGAV operation

Here, cutplanes across the intake and exhaust are shown, revealing the air/fuel ratio (lambda) throughout the cylinder. At 180° b.TDC the mixture appears heterogeneous, especially in the cutplane I – E ii. The rich area shown on the left of the plane corresponds to the area of high methane concentration under the intake valve closest to the intake manifold as seen in figure 13. Both cutplanes exhibit a diagonal flow from top to bottom which develops into vortices that spin in differing directions, further homogenising the mixture. By 10° b.TDC, these vortices have disappeared and a more linear flow, normal to the piston bowl is observed, moving upwards to the cylinder head. The mixture is well homogenised, although a slightly richer area remains under the intake valve in cut I – E ii.

The homogenisation is made further visible in figure 15.

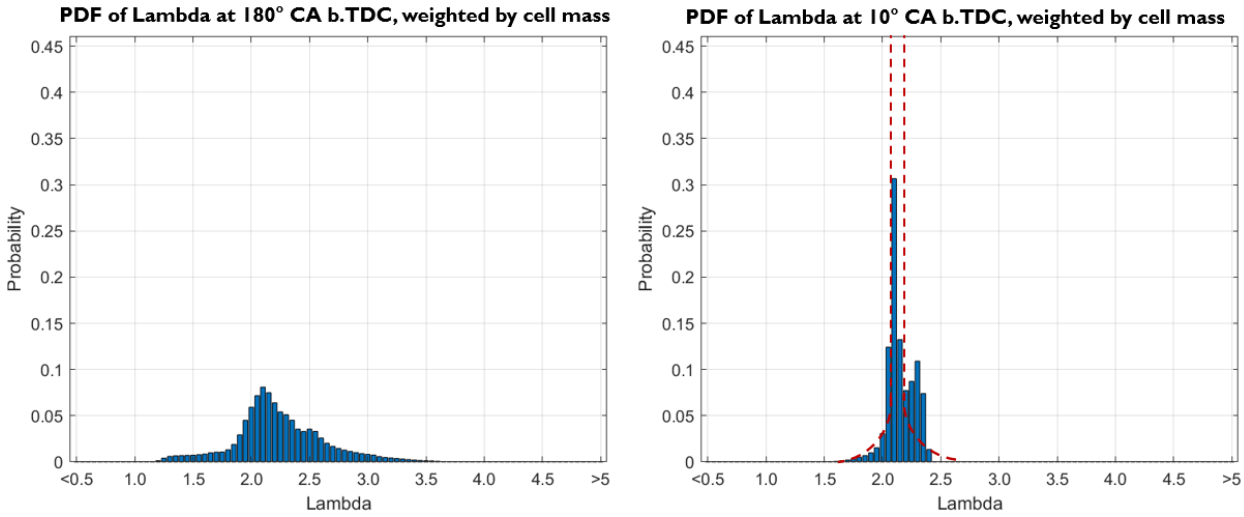

Figure 15: Lambda distribution at 180° and 10° b.TDC, low pressure SOGAV operation

These plots reveal the lambda value of each cell in the simulation. The cells were weighted by mass to counteract the effects of differing cell sizes in the domain and in the two different meshes show. From this information, the probability of lambda being a certain value can be ascertained, as is shown in figure 15. The red dashed line in the right hand plot indicates how a near - perfect homogenisation would appear, with nearly all cells having the global lambda value of 2.2. At 180° b.TDC, the lambda values range from 1.2 to 3.6. The distribution exhibits a peak at al lambda value of 2.1, with 8% of cells having this value. The results of the homogenisation processes during the compression stroke can clearly be seen at 10° b.TDC, where 31% of all cells in the domain are filled with a mixture of air and fuel at lambda 2.1. The span of lambda values has decreased, the lowest lambda value being 1.6, the highest being 2.4. The mixture is well, although not perfectly homogenised before the start of combustion which took place at 5° b.TDC in the experiment.

The following section examines if a similar level of homogeneity is possible using a medium pressure direct gas injector.

4.5. Homogenous Medium Pressure DI Operation

One of the main benefits of using direct injection is the possibility of eliminating methane slip resulting from methane residing in the intake manifold being lost through the exhaust valve during valve overlap. Using direct injection after exhaust valve closing results in extremely low levels of methane in the intake, as a minimal amount of the fuel adheres to the cylinder head due to the coandă effect and can enter the intake manifold towards the end of the intake stroke where the pressure difference between intake and cylinder is not so high.

If the injection window takes place after intake valve closing, methane in the intake manifold can be avoided altogether. This comes at the price of time available for homogenisation and the inability of using the turbulence in the intake stroke to homogenise the mixture.

In order to highlight the differences and benefits of medium pressure direct injection, simulations were carried out at 100% load, using the same boundary conditions as for low pressure SOGAV operation.

Table 3 shows the injection parameters used for the two simulations.

Table 3: Injection parameters for medium pressure direct injection

Parameter	Simulation 1	Simulation 2	Unit
Engine operating point	100	100	%
Start of injection	320	205	° b.TDC
Injection duration	30	30	° CA
Injected methane mass	3550	3550	mg

The start of injection in simulation 1 is 320° b.TDC, 5° CA after exhaust valve closing, ensuring no methane is lost through the exhaust valve.

The start of injection for the serial low pressure SOGAV operation is 361° b.TDC. For simulation one, this means that 41° CA are lost for homogenisation processes. However, the injection takes place more rapidly, ending only 5° CA after the SOGAV injection. The injected methane mass for SOGAV operation, simulation 1 and simulation 2 is identical.

In simulation 2, methane is first injected when the intake valve is closed, meaning a loss of 156° CA for homogenisation.

The direct injector is provided with a jet-forming ring. The following simulations were performed without this ring, allowing a higher homogenisation due to the wider spread of the hollow cone methane injection.

Figure 16 shows the injection of methane into the cylinder for both simulations.

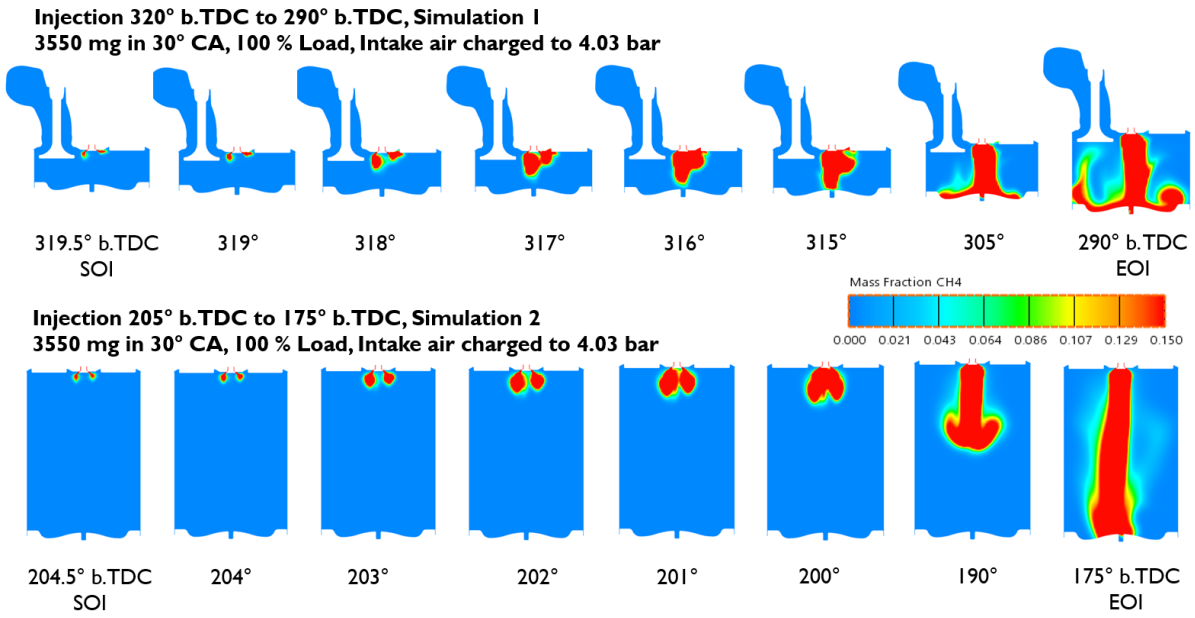

Figure 16: Direct injection of methane into the engine cylinder

In both scenarios, the fuel begins to propagate as a wide ring injection before collapsing to a narrow jet due to the area of low pressure underneath the poppet valve. This behaviour of gas injection from a poppet style valve is corroborated by [5]. The later injection (simulation 2) takes slightly longer to

collapse, in this case around 5° CA. In simulation one, the incoming stream of intake air deforms the jet, causing it to initially bend away from the intake valve. This also results in an earlier collapse, only 4° CA after SOI. Due to the piston position at the time of injection, the fuel hits the piston bowl earlier in simulation one, after which it follows the contour of the bowl towards the cylinder walls. The required injection pressure for both scenarios is 53 bar.

The benefit of fuel injection during the intake stroke (simulation 1) is that the turbulence created by the inflow of air through the intake valve can be utilised for the mixing of air and fuel. The disadvantage is the possibility of methane entering the intake manifold. The simulation revealed that a mere 9.14 $x10^{-12}$ mg of methane are present in the intake manifold at intake valve closing, a negligible amount, making this a viable injection strategy for medium pressure operation. Figure 17 shows the homogenisation during the compression stroke.

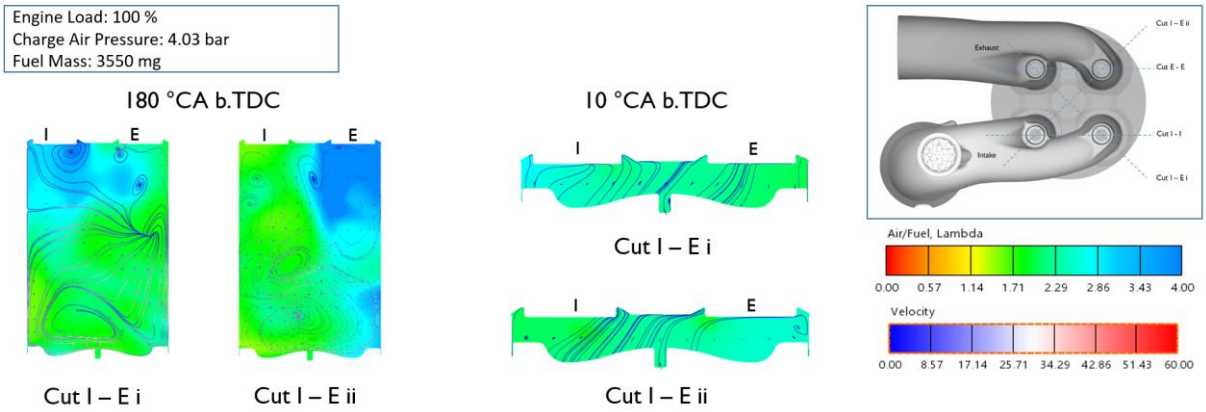

Figure 17: Cutplanes showing lambda during the compression stroke, Injection 320° - 290 °b.TDC

These cutplanes show the air/fuel ratio, lambda, at the start and end of compression. At 180° CA the mixture of gas and air is already well mixed due to the turbulence of the intake air flow. There are lean areas under the intake valve furthest from the intake manifold and under the exhaust valve furthest from the exhaust manifold. Although the mixture is well homogenised by 10° b.TDC, these areas remain slightly leaner. The flow patterns are similar to those found in the low pressure SOGAV operation, although not identical. The degree of homogenisation can be seen in figure 18.

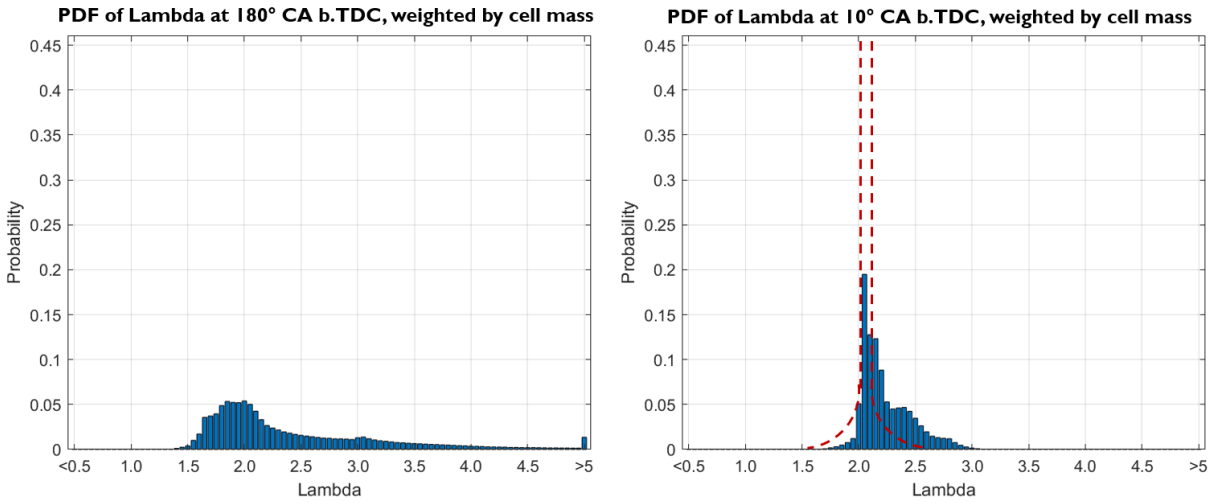

Figure 18: PDF of lambda at the start and end of compression, injection 320° - 290° b.TDC

Although homogenisation is evident, the mixture is more heterogeneous than with low pressure SOGAV operation due to the lesser time available. At 10° b.TDC, 19% of cells in the simulation have a lambda value of 2.1 in comparison to the 31% found in the simulation with SOGAV injection. Lambda ranges from 1.7 to 3.0, meaning that the mixture is easily combustible however.

In simulation 2, fuel was injected after intake valve closing in order to eliminate methane entering the intake manifold. This makes for a greater heterogeneity, as seen in figure 19.

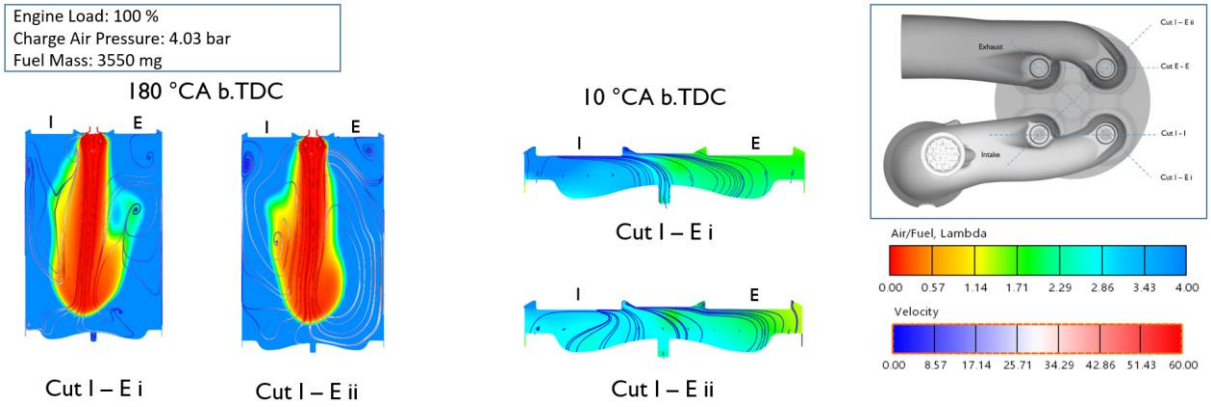

Figure 19: Cutplanes showing lambda during the compression stroke, Injection 205° - 175 °b.TDC

At 180° the gas injection is still taking place, shown by the incredibly rich area emanating from the centrally mounted gas injector. The downwards directed injection has a strong effect on the cylinder flow, making the flow field much different than previously observed. The gas and air mixture moves downwards until the piston bowl is hit, where it recirculates upwards before being re-entrained in the downwards flow. The mixture at 10° b.TDC is significantly more heterogeneous. The areas under the intake valves are leaner, whereas a richer mixture is found under the exhaust valves. These findings are reciprocated by the lambda distribution plots seen in figure 20.

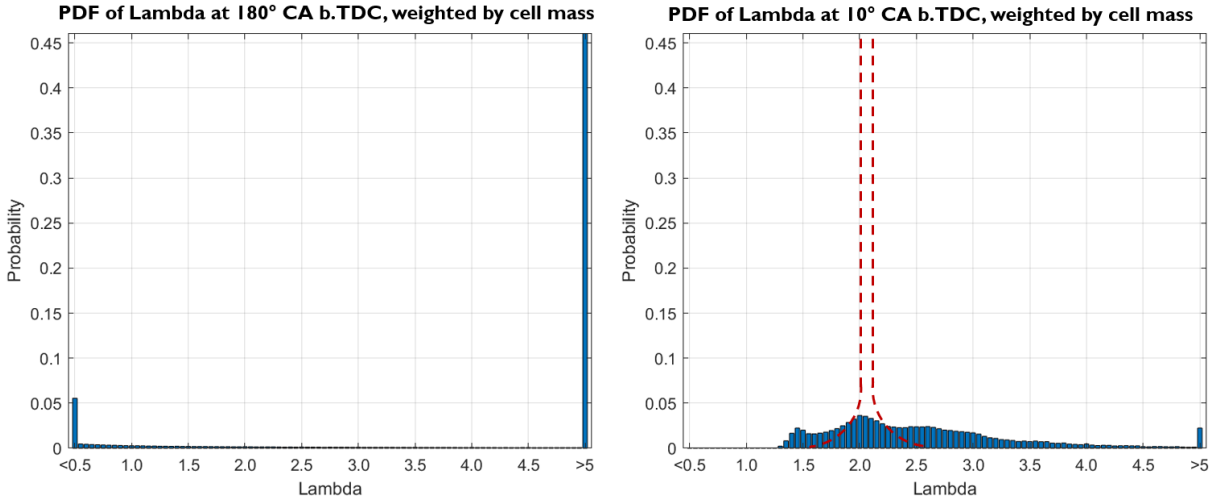

Figure 20: PDF of lambda at the start and end of compression, injection 205° - 175° b.TDC

The lambda distribution at 180° CA b.TDC reveals that no significant mixing has taken place during the injection. The cells are divided into extremely rich (5.5%) and extremely lean areas (80.5%). The remaining 14% represent cells where some mixing has occurred. The compression stroke is now the

only time available for mixing, resulting in a lower degree of homogenisation as seen at 10° b.TDC. Although there is a small peak (3.6% of all cells) at the lambda value 2.0, lambda is well distributed between 1.3 and >5. The lambda values are however generally within the combustibility limits for methane. Due to the increased number of rich cells and the heterogeneous mix, engine knock could become more prevalent using this injection strategy. A proved method for controlling engine knock is the use of stratified charge engine operation modes.

4.6. Stratified Charge Operation

Two stratified charge modes are presented here. The first, known from spark ignited engines to combat engine knock, consists of an early injection to create a lean homogenous mixture, followed by a late injection creating a rich area in the centre of the piston bowl. The homogenous mixture is too lean for knock to occur. Combustion speed is increased when burning from rich to lean areas ensuring the fuel-air mix burns throughout. It is beneficial that the fuel is more centred within the combustion chamber, meaning that less wall quenching occurs.

The second method consists of injecting the entire fuel in a late injection and trapping it within the piston bowl and centre of the cylinder.

Both methods are useful for reducing methane slip, as there is less wall quenching.

In order for these methods to work, a suitable piston crown must be chosen that is able to retain the fuel in the centre of the cylinder. One such piston geometry, an experimental high-squish piston available at the University of Rostock, is shown in figure 21, depicting lambda over the course of the two injections of method 1.

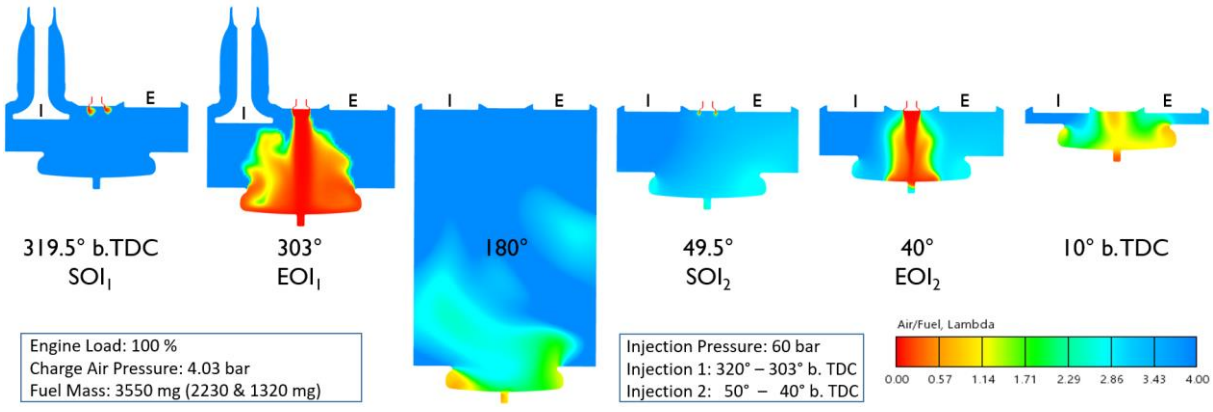

Figure 21: Stratified charge operation using two injections

The injector's jet-forming ring was installed for these simulations, creating a compact jet of fuel with rapid, targeted cylinder penetration. The fuel mass is divided into two shots, the first and larger delivering 2230 mg of methane in 17° CA starting at 320° b.TDC. This results in a global lambda of 3.5, a very lean mix that will not be prone to knocking. The second injection takes place at 50° b.TDC, delivering 1320 mg of fuel in 10° CA. The injection pressure is 60 bar and the injection is supercritical. The result can be seen at 10° b.TDC – a heterogeneous rich mix in the centre of the piston bowl and a lean mix at the piston walls. The global lambda value is now 2.2. The development of the lambda distribution is presented in figure 22.

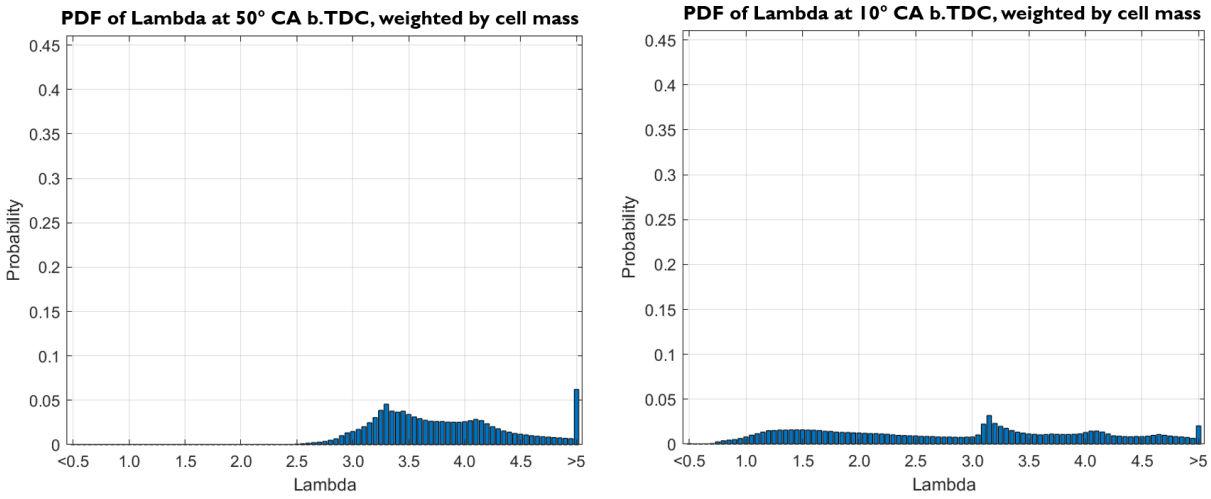

Figure 22: Development of lambda distribution between SOI_2 and 10° CA b.TDC

Although the first injection took place at the same time as simulation one in 4.5, the homogenisation is much lessened due to the geometry of the piston bowl, which tends to retain the gas and not recirculate it into the cylinder air. There is a peak (4.6%) at a lambda value of 3.35, and another (6%) at lambda greater than five. The richest lambda values represented occur at lambda 2.5. This lean mixture should guarantee an extremely low knock level. After the second injection from 50° - 40° b.TDC, mixing processes continue, producing a wide banded heterogeneous mix at 710° b.TDC, ranging from lambda values of 0.7 to greater than 5. This mixture should offer good combustion with low knock potential due to the decreased time in which rich mixtures are present in the cylinder and with the added advantage that less fuel is near the cylinder walls, increasing combustion efficiency and decreasing methane slip due to incomplete combustion.

Alternatively, a stratified charge can be achieved using a single late injection, as seen in figure 23.

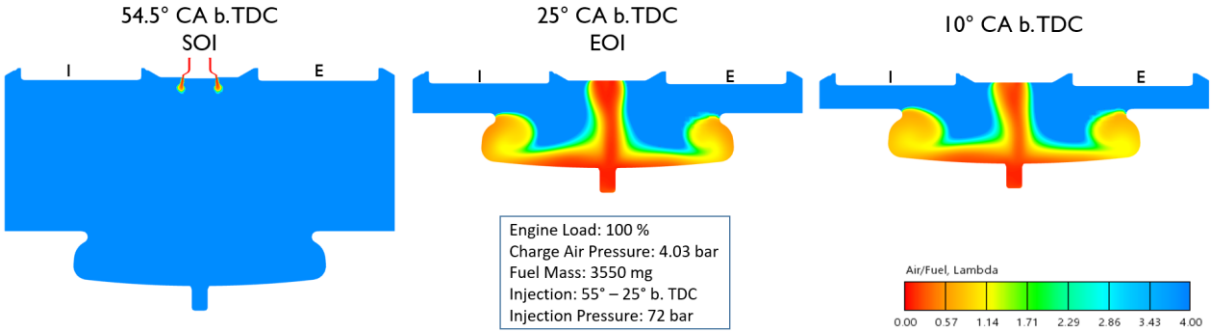

Figure 23: Stratified charge operation using a single injection

The jet-forming ring creates a rapid penetrating jet of methane which hits the piston crown and then follows its contour, creating a vortex around the outer edge of the piston bowl. The Coandă effect can be observed here, as the methane adheres to the engine head long after the end of injection at 25° CA b.TDC. At 10° CA b.TDC, a heterogeneous mix is present within the piston bowl, the richest areas being directly in contact with the piston. The bore used for mounting the piston (centre of piston bowl) is filled with methane. If the piston is not sufficiently warm, quenching effects could cause a rise in methane slip due to incomplete combustion in the proximity of the piston and within the piston mounting bore.

The lambda distribution for this operation mode is shown in figure 24.

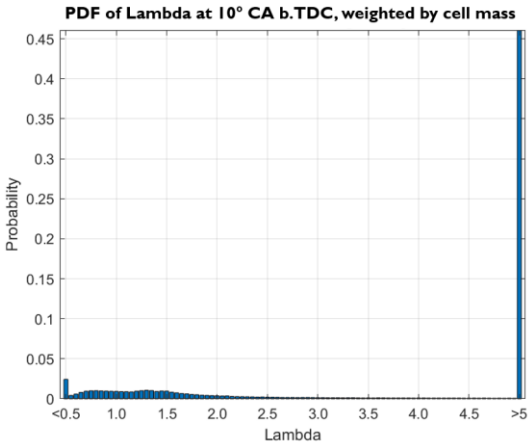

Figure 24: Lambda distribution at 10° CA b.TDC, single injection stratified charge

The distribution can be divided into a rich area with lambda values smaller than 0.5 up to lambda values around 2.5, and lean area in which little or no methane is present. The peak in the rich area occurs for lambda values smaller than 0.5 and speaks for 2.4% of the cells in the simulation. The major peak occurs in the lean area, with 65% of cells having a lambda value of five or greater.

Although the mixture is well positioned in the piston crown, the extremely rich lambda areas in close proximity to the piston could result in poor combustion behaviour.

To highlight the differences in these two approaches, the amount of fuel in different areas of the cylinder was calculated, as seen in figure 25.

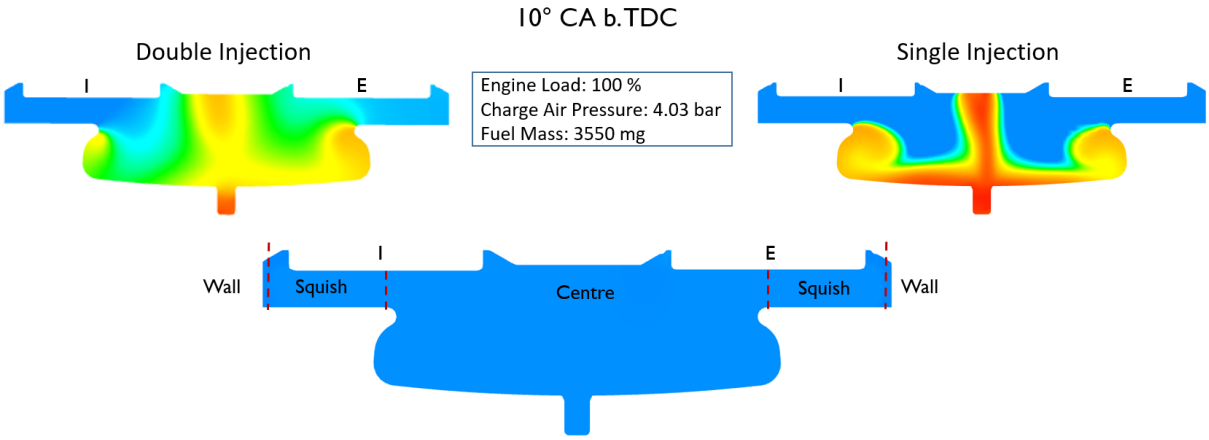

Figure 25: Comparison of methane distribution within the cylinder: double vs. single shot injection

The cylinder was divided into the central area above the piston bowl (radius, r < 104 mm), the squish area (104 mm< r < 166 mm), and a near-wall area (r > 166 mm). The piston has a diameter of 340 mm. The results of the methane distribution analysis are presented in table 4.

Table 4: Methane distribution in the engine cylinder

Operation Mode	**Double Injection Stratified**		**Single Injection Stratified**		**SOGAV Homogenous**	
	Mass CH4 in [mg]	%	**Mass CH4 in [mg]**	%	**Mass CH4 in [mg]**	%
Centre	2630.18	74.09	3315.88	93.4	2673.89	75.32
Squish	866.03	24.4	234.12	6.59	740.05	20.85
Wall	53.79	1.51	1.16×10^{-7}	3.26×10^{-9}	136.06	3.83
Total	3550	100	3550	100	3550	100

In comparison to homogenous operation with SOGAV injection, using a double shot stratified injection decreases the near-wall methane by 50%. Using a single shot injection as detailed eradicates near-wall methane.
The mass of methane in the centre of the piston bowl is very comparable for the double injection and homogenous operation. In the single injection simulation, this is almost 20% higher.

The mass of methane retained in the intake manifold was also calculated and is presented in the next section.

4.7. Comparison of Operation Modes: Methane Present in the Intake Manifold

A comparison of the methane present in the intake manifold at intake valve closing for the differing operation modes is presented in table 5.

Table 5: Methane present in the intake manifold at intake valve closing

Injection Strategy	Injector	CH4 in Intake Manifold at IVC	Unit
Low pressure PFI 100 %	SOGAV	376.1	mg
Low pressure PFI 50 %	SOGAV	183.5	mg
Medium pressure injection after EVC, 100 %	DI	9.14 e-12	mg
Medium pressure injection after EVC, 50 %	DI	5.57 e-13	mg
Medium pressure injection after IVC	DI	0	mg
Stratified charge methods	DI	0	mg

According to the simulation, 10.6% of the total fuel remains in the intake using the serial SOGAV injection strategy (10.3% at 50% load). This methane will enter the cylinder in the next cycle and either be lost via the exhaust valve or combusted with the fresh charge. Reducing the amount of methane in the intake will drastically reduce methane slip and could lead to better performance as cyclical fluctuations and knock potential will also be reduced. Using direct injection in the intake stroke after

exhaust valve closing reduces methane in the intake to negligible amounts. Injecting the methane into the cylinder after intake valve closing eliminates methane in the intake completely.

5. Conclusion and Outlook

The aim of this paper was to present ways in which using a methane direct injector could improve methane slip.

Using direct injection in the intake stroke after exhaust valve closing reduces methane in the intake to negligible amounts and provides a good level of homogenisation. The lambda values present in the cylinder range between 1.7 and 3.1 whereas the serial SOGAV strategy results in a lambda range from 1.7 to 2.4, showing that engine knock should not be significantly increased as richer areas are not prevalent in the more heterogeneous mixture produced by the DI strategy. There is also potential for performance increase using DI, as no air is displaced by the methane in the intake manifold. As methane is not lost to the exhaust, fuel economy is also increased.

Further retarding the injection timing to after IVC reduces methane in the intake to zero, but at the cost of a much more heterogeneous mixture due to not being able to utilise the turbulence caused by the intake air for mixing purposes. Richer areas are prevalent which could lead to higher knock levels.

As knock is a function of time, reducing the time in which the fuel is in the cylinder is one way of combatting knock, as seen in the stratified charge single injection strategy. Here the fuel was injected late in the compression stroke. Depending on the piston bowl geometry, this could lead to unburned methane due to very rich areas close to the piston surface. There will be no wall quenching along the cylinder wall, as next to no methane resides here.

Using a double injection strategy, the first injection to create a lean basic mixture and the second late in the compression stroke, a similar distribution of methane can be obtained as in homogenous SOGAV operation, but with 50% less methane in the near-wall area. The mixture is however much more heterogeneous.

The effect of these operation modes on combustion are yet to be analysed with the parameterisation of the combustion equations. This requires engine data which will be produced in the following months. Nevertheless, the simulated results show promise for eliminating methane slip by shortcutting and for decreasing the near-wall methane, leading to less wall-quenching.

If the costs of gas compression are outweighed by the benefits of low methane slip operation with improved combustion efficiency, medium pressure direct injection on dual-fuel marine engines could prove very effective at bridging the gap between the fuel market of today and tomorrow.

Acknowledgements

The authors would like to thank the Federal Ministry for Economic Affairs and Climate Action for funding the project 'TEME 2030+' (project number: 03SX537A). Furthermore, our thanks go to FVTR GmbH, Schaller Automation GmbH & Co. KG, KS Kolbenschmidt Large Bore Pistons GmbH, Kompressorenbau Bannewitz GmbH, M. Jürgensen GmbH und Co. KG, SICK AG und Umicore for supporting this project.

Supported by:

Federal Ministry for Economic Affairs and Climate Action

on the basis of a decision by the German Bundestag

Literature

[1] Hanjalic, K., Popovac, M., Hadziabdic, M. "A robust near-wall elliptic-relaxation eddy-viscosity turbulence model for CFD", Int. J. Heat Fluid Flow, 25, 1047–1051, 2004.

[2] Schiller, L. and Naumann, A. "A Drag Coefficient Correlation." Zeitschrift des Vereins Deutscher Ingenieure, 77, 318-320, 1935

[3] Dukowicz, J.K. "Quasi-steady droplet change in the presence of convection", informal report Los Alamos Scientific Laboratory, LA799MS, 1979

[4] Di Modica, D.V. "Numerische Untersuchung der Zylinderinnenströmung eines mittelschnelllaufenden Verbrennungsmotors", Masterthesis, TU Braunschweig, 2017

[5] Deshmukh et al. "Characterization of Hollow Cone Gas Jets in the Context of Direct Gas Injection in Internal Combustion Engines", SAE International, 2018, doi: 10.4271/2018-01-0296